Vacuum 87 (2013) 81–83

Contents lists available at SciVerse ScienceDirect

Vacuum

journal homepage: www.elsevier.com/locate/vacuum

Rapid communication

(001) CeO_2 films epitaxially grown on $SrTiO_3$ (001) substrates by pulsed laser deposition using a metallic Ce target

Haiping Wang [a,*], Hongliang Zhang [b], Hui Zhang [a], Junfeng Bai [a], Jiashun Ren [a], Shengjiang Wang [a]

[a] China Maritime Police Academy, Ningbo 315801, PR China
[b] Ningbo Institute of Material Technology and Engineering, Chinese Academy of Sciences, Ningbo 315201, PR China

ARTICLE INFO

Article history:
Received 15 June 2012
Received in revised form
21 July 2012
Accepted 21 July 2012

Keywords:
Cerium dioxide
Pulsed laser deposition
Epitaxial growth
Thin films

ABSTRACT

Cerium dioxide (CeO_2) films have been epitaxially grown on $SrTiO_3$ (001) substrates by pulsed laser deposition using a metallic Ce target in oxygen ambient. *In situ* reflection high energy electron diffraction and X-ray diffraction confirm the formation of epitaxial (001) oriented CeO_2 phase. Atomic force microscope and Raman spectra were used to characterize the surface morphologies and the bonding structures of the CeO_2 films. Epitaxial growth of thick CeO_2 films contributes chiefly to a uniform and smooth surface with root mean square roughness of up to 0.272 nm and a high-symmetry F_{2g} mode.

Considerable attention has been paid to the research of cerium dioxide (CeO_2) thin films for more than a decade, because CeO_2 is an important material with a wide variety of technological applications, such as catalysis, fuel cells, sensors, microelectronics, optical coatings and films [1,2].

This lattice parameter match or mismatch is an important factor in thin film growth. Cubic fluorite and perovskite CeO_2 having an excellent lattice matching with $SrTiO_3$ by rotation 45° along the (001) direction can be epitaxially grown on $SrTiO_3$ (001) substrates by molecular-beam epitaxy [3]. Also, by simply rotation 45° in the CeO_2 basal plane, the lattice mismatch will be 0.16% and 1.7% along *a* and *b* axis of (YBCO), respectively. CeO_2 is one of the most promising buffer layers and diffusion barriers in the growth of high-temperature superconductors such as $YBa_2Cu_3O_{7-\delta}$ (YBCO) [4,5]. It is important to obtain (001) oriented CeO_2 in order to grow c-axis oriented epitaxial YBCO films [6,7]. Pulsed laser deposition (PLD) can provide a convenient route to achieve YBCO/CeO_2 heteroepitaxial layers [8]. As recently stated by Magdalena Klimczak-Chmielowska et al. [1], the thin film formation process in PLD can be divided into the following four steps: (i) laser radiation interaction with the target; (ii) dynamic of the ablated materials; (iii) deposition of the ablated materials on the substrate; and (iv) nucleation and growth of a thin film on the substrate surface. Among them, i and ii, namely laser radiation with the target and dynamic of the ablated materials, are key factors that influence the quality of the thin films. Using a metallic target, the high quality metallic oxide films were grown by PLD method in optimum condition due to single metallic bond (relatively less covalent bond) ablated by laser and a lower ablation fluence [9,10]. Usually, the CeO_2 films are obtained using a CeO_2 target [11], but the technique has such disadvantages of CeO_2 target over Ce metallic target as more particles in the plasma and higher ablation fluence, which greatly limited the potential application of epitaxial CeO_2 films in many fields. To avoid these disadvantages of epitaxial growth of CeO_2 films, we have recently developed a variant technique in which the CeO_2 films are grown using a metallic target.

In this letter, (001) oriented CeO_2 films first epitaxially grown on the $SrTiO_3$ (001) substrates by PLD using a metallic Ce target in the background gas of O_2. The crystalline characteristics, growth mechanism, surface morphologies, and bonding structures of the CeO_2 films were investigated.

The CeO_2 films were prepared on the $SrTiO_3$ (001) substrates by PLD using a metallic Ce target in the oxygen ambient. The metallic Ce target was rotated during the ablation process to reduce the possible nonuniform erosion, which is the optimum distance of about 60 mm away from the substrates for epitaxial growth of CeO_2 films. Oxygen gas was supplied into the chamber at a flow rate of 5 sccm. The films were deposited in the background pressure of $\sim 2 \times 10^{-6}$ Pa and experimental pressure of $\sim 5 \times 10^{-5}$ Pa. Plasma was produced between the $SrTiO_3$ substrate and the metallic Ce

* Corresponding author. Tel./fax: +86 574 86165529.
E-mail address: 123-whp@163.com (H. Wang).

0042-207X/$ – see front matter
http://dx.doi.org/10.1016/j.vacuum.2012.07.012

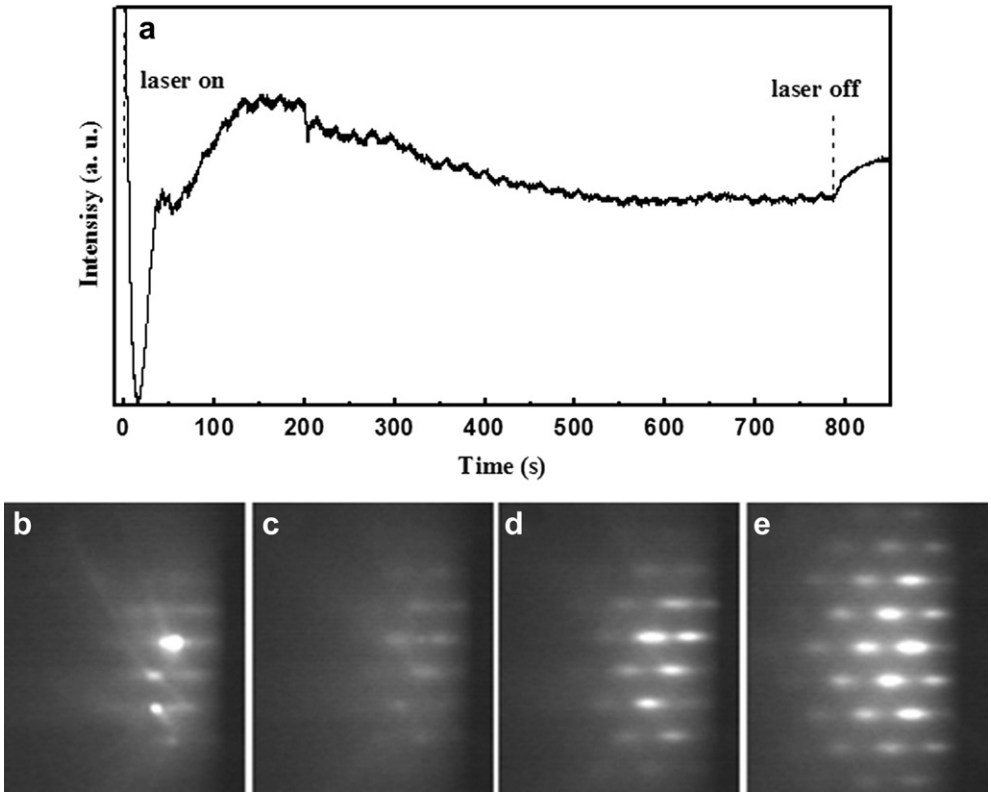

Fig. 1. (a) Typical RHEED intensity oscillation recorded on streak during the CeO_2 epitaxial growth. Typical RHEED patterns collected at (b) 0 s, (c) 15 s, (c) 170 s and (e) after deposition.

target using a focused KrF (248 nm) laser with an energy density of ~1.5 J/cm^2 and a repetition rate of 1 Hz. The substrate temperature was kept at approximately 500 °C during deposition. The crystallinity of the surfaces of the as-grown films was probed *in situ* by reflection high energy electron diffraction (RHEED). The surface morphologies and structures of the films were analyzed *ex situ* by atomic force microscope (SEIKO SPA-300HV) and X-ray diffraction (XRD, X'Pert Pro with Cu-K_α radiation source), respectively. Raman spectra (exited by 528 nm, in Via made in Renishaw Corporation) were used to characterize the bonding structures of the CeO_2 films.

Fig. 1(a) shows the intensity variation of RHEED specular beam spot during CeO_2 film growth on $SrTiO_3$ (001) substrate using the metallic Ce target in the oxygen ambient. Due to the layer-by-layer epitaxial growth of the CeO_2 film, the periodic intensity oscillation curve was observed. One period of oscillation corresponds to the growth of one unit cell of CeO_2. The growth rate is estimated to be 0.0483 monolayer (ML)/s by the analysis of the oscillation period, where 1 ML corresponds to a layer thickness of 0.541 nm, the value of the *c*-axis lattice constant of the bulk CeO_2. As shown in Fig. 1(a), the oscillatory behavior can persist up to about 35 cycles corresponding to 18.9 nm. The thickness of the CeO_2 film is about 150 nm determined by calculation and analysis of the *in situ* RHEED intensity oscillation. Fig. 1(b)–(e) shows typical RHEED patterns collected at 0 s, 15 s, 170 s and after deposition, respectively. In order to give evolution of epitaxial growth of the CeO_2 film, the RHEED pattern of $SrTiO_3$ (001) substrate surface collected before deposition is shown in Fig. 1(b). As soon as the deposition started, the superstructures of the $SrTiO_3$ (001) surface vanished. The streaks were clearly observed throughout the deposition of the CeO_2 film as thick as 150 nm. The RHEED pattern shown in Fig. 1(e) is taken from the film after deposition, which is a perfect CeO_2 (001) single crystal pattern of <011> azimuth without extra spots and has short streaks, indicating that the sample is high-quality single crystalline CeO_2 (001) layer. The patterns collected in the period (after deposition) remained to be streaky, indicating that the surface was atomically smooth with a layer-by-layer growth. Epitaxial CeO_2 films grown using a CeO_2 ceramic target have a layer-by-layer growth mode up to a thickness of 100 nm [12]. The alternative method of using a metallic Ce target can take advantage of a layer-by-layer growth of CeO_2 films.

Fig. 2(a) shows the X-ray diffraction θ–2θ scans of the CeO_2 film on the $SrTiO_3$ (001) substrate. Only the (002) and (004) peaks of the CeO_2 film appear in the diffraction patterns, indicating that the

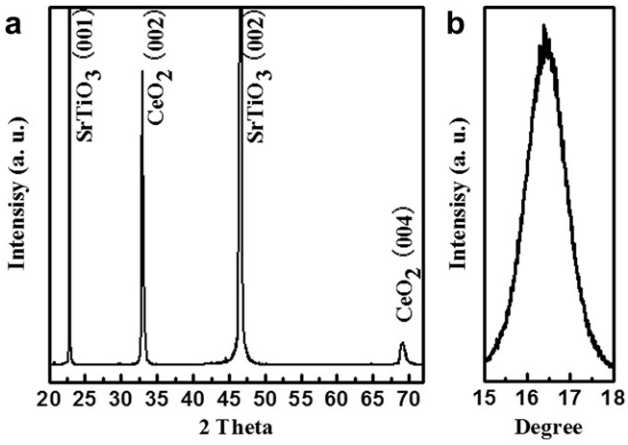

Fig. 2. (a) XRD pattern of the CeO_2 film on the $SrTiO_3$ substrate and (b) X-ray rocking curve for (002) reflection of the CeO_2 film.

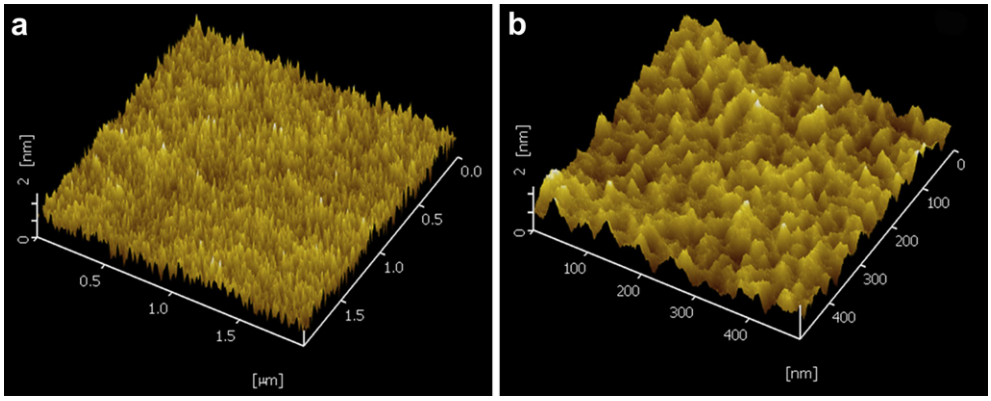

Fig. 3. AFM images of the CeO_2 film taken over scan areas of (a) $2 \times 2\ \mu m^2$ and (b) $500 \times 500\ nm^2$.

CeO_2 film is basically c-axis oriented. X-ray rocking curve for (002) reflection of the CeO_2 film is shown in Fig. 2(b). The rocking measurement of the CeO_2 film grown using the metallic Ce target in the oxygen ambient reveals that the width at half maximum is found to be 0.97°, suggesting that the CeO_2 film has good single crystallinity. The laser absorption in metallic targets is higher than that in dielectric targets. The total number of electrons emitted from metallic targets is more than that from dielectric targets and the hot electron temperature in metallic targets is higher than that of dielectric targets [13]. Since a method of using a metallic Ce target change the laser absorption, the total number of electrons and the hot electron temperature in a metallic Ce target, the structural perfection of the epitaxial CeO_2 film seems to be dependent on the method of using a metallic Ce target. This new alternative method of using a cerium metallic target, as compared to ceramic target, allows a better control of the cerium oxidation and leads to good structural properties that can be used to many interesting oxides such as ZnO, VO_2, WO_3, or TiO_2 [14]. The thick *c*-axis oriented CeO_2 epitaxial film is a potential application for the growth of *c*-axis oriented epitaxial YBCO films.

AFM images of the CeO_2 film is shown in Fig. 3. In order to verify the layer-by-layer growth, two different areas of the film surface were selected to take pictures. The surface of the film is uniform and smooth, and the root mean square values are 0.272 nm and 0.271 nm for scan areas of $2 \times 2\ \mu m^2$ and $500 \times 500\ nm^2$, respectively. The almost same root mean square values of two different areas are attributed to the epitaxial growth along *c*-axis oriented CeO_2.

Fig. 4 shows the Raman scattering spectra of the CeO_2 film. The sharp peak at 464 cm^{-1} is attributed to symmetric F_{2g} mode [15]. And the weak peaks at around 120, 246, 321, 622, 670 and 1605 cm^{-1}, as shown in the red plotting, are due to the Raman active modes of the $SrTiO_3$ substrate. The high intensity of the peak corresponds to the best quality films deposited at the optimum growth condition, which is consistent with the *in situ* RHEED and X-ray diffraction results. However, the peak is slightly shifted with respect to those of the single crystal and its FWHM is slightly broad. This is crystal distortion caused by the lattice mismatch between the CeO_2 film and the $SrTiO_3$ substrate.

Epitaxial CeO_2 films were grown on the $SrTiO_3$ (001) substrates by PLD using the metallic Ce target. The *c*-axis oriented CeO_2 epitaxial growth is identified by the *in situ* reflection high energy electron diffraction and X-ray diffraction. Epitaxial growth of 150-nm-thick CeO_2 films contributes chiefly to a uniform and smooth surface with root mean square roughness of up to 0.272 nm. The high-symmetry F_{2g} mode is determined by the structural perfection of the films. The thick c-axis oriented CeO_2 epitaxial film is a potential application for the growth of *c*-axis oriented epitaxial YBCO films.

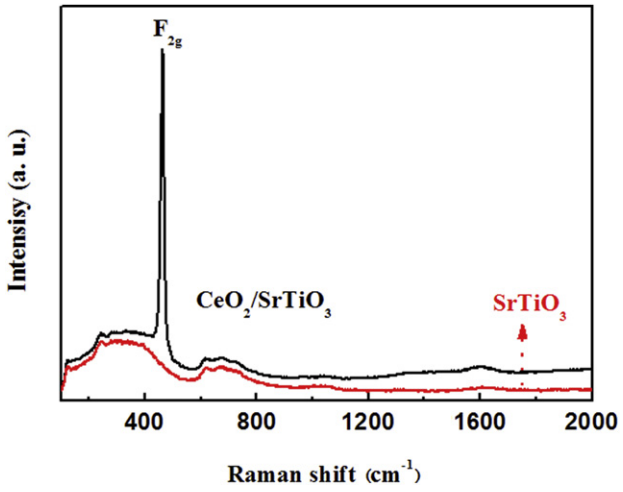

Fig. 4. Raman spectra (528 nm excitation) of the CeO_2 film.

References

[1] Klimczak-Chmielowska Magdalena, Chmielowski Radoslaw, Kopia Agnieszka, Kusinski Jan, Villain Sylvie, Leroux Christine, et al. Thin Solid Films 2004;458:98–107.
[2] Rexer Eric F, Wilbur Donald B, Mills Jeffrey L, DeLeon Robert L, Garvey James F. Rev Sci Instrum 2000;71:2125–30.
[3] Uedono A, Shimoyama K, Kiyohara M, Yamabe K. J Appl Phys 2003;94:5193–8.
[4] Bhuiyan MS, Paranthaman M, Sathyamurthy S. Supercond Sci Technol 2003;16:1305–9.
[5] Abiade Jeremiah T, Oh Sang Ho, Kumar Dhananjay, Varela Maria, Pennycook Stephen, Guo Haizhong, et al. J Appl Phys 2008;104:073910.
[6] Wu XD, Dye RC, Muenchausen RE, Foltyn SR, Maley M, Rollett AD. Appl Phys Lett 1991;58:2165–7.
[7] Reade RP, Church SR, Russo RE. Rev Sci Instrum 1995;66:3610–4.
[8] Boikov Yu A, Claeson T, Erts D, Bridges F, Kvitky Z. Phys Rev B 1997;56:11312–9.
[9] Hino T, Nishida M, Araki T. Surf Coat Technol 2002;149:1–6.
[10] Mendelsberg RJ, Kerler M, Durbin SM, Reeves RJ. Superlattices Microstruct 2008;43:594–9.
[11] Koinuma Hideomi, Nagata Hirotoshi, Tsukahara Tadashi, Gonda Satoshi, Yoshimoto Mamoru. Appl Phys Lett 1991;58:2027–9.
[12] Shi DQ, Ionescu M, Silver TM, Dou SX. Physica C 2003;384:475–81.
[13] Chen LM, Zhang J, Teng H, Dong QL, Chen ZL, Liang TJ, et al. Phys Rev E 2001;63:036403.
[14] Fouchet A, Prellier W, Mercey B, Méchin L, Kulkarni VN, Venkatesan T. J Appl Phys 2004;96:3228–33.
[15] Weber WH, Hass KC, McBride JR. Phys Rev B 1993;48:178–85.